Dynamic Structure Factor of Disordered Quantum Spin Ladders

Max Hörmann,* Paul Wunderlich,† and K. P. Schmidt‡
Institute for Theoretical Physics, FAU Erlangen-Nürnberg, 91058 Erlangen, Germany

(Received 5 June 2018; published 16 October 2018)

We investigate the impact of quenched disorder on the zero-temperature dynamic structure factor of two-leg quantum spin ladders. Using linked-cluster expansions and bond-operator mean-field theory, huge effects on individual quasiparticles but also on composite bound states and two-quasiparticle continua are observed. This leads to intriguing quantum structures in dynamical correlation functions well observable in spectroscopic experiments.

DOI: 10.1103/PhysRevLett.121.167201

Disorder is an inevitable ingredient of any condensed matter. On the one hand disorder can change or even destroy the physical behavior of the associated clean systems [1–3] or, on the other hand, it can induce fundamentally new physics. This is especially true for correlated quantum materials where the interplay of disorder and quantum fluctuations can result in technological challenges or exotic phases of quantum matter like many-body localization [4–7]. One important aspect in the collective behavior of correlated quantum matter is the formation of quasiparticles and their role in quantum critical behavior. While many studies have investigated the static and thermodynamic properties of such systems in the presence of disorder [8–16], the fate of interacting quasiparticles under disorder is only rarely studied. Experimentally, however, increasingly improving resolution in spectroscopy like inelastic neutron or light scattering as well as intentional doping to control disorder in quantum materials [17–24] demands theoretical predictions for dynamical correlation functions of correlated quantum matter in the presence of disorder.

An outstanding arena, both experimentally and theoretically, to investigate the influence of quenched disorder on quasiparticle excitations are low-dimensional quantum magnets, which host a variety of interesting quantum phases and elementary particles in the clean case. Theoretically, the calculation of dynamical correlation functions for disordered quantum magnets is challenging [25–27]. Only recently [26] the effect of disorder on single quasiparticles has been studied within bond-operator mean-field (MF) theory for the bilayer square lattice Heisenberg model, but the fate of quasiparticles under disorder beyond MF theory is largely unexplored.

Particularly promising systems to advance are antiferromagnetic two-leg quantum spin ladders (QSLs) [28], which have been investigated successfully over the last decades in a number of experimental realizations [29–35] and by various theoretical tools [36–41]. Clean QSLs have non-ordered ground states and gapped triplon excitations [37,42]. Inelastic neutron and light scattering allow us to access one-triplon dispersions but also the formation of two-triplon bound states and continua reflecting the presence of large quantum fluctuations. Furthermore, it is possible experimentally to intentionally dope QSL compounds so that quenched disorder is induced into the system, either by site disorder [43] or bond disorder [44]. It is therefore important to understand the influence of disorder on the spectral signatures of triplon quasiparticles in QSLs. To this end quenched bond disorder is optimal, since the types of magnetic interactions are unchanged. This is exactly the punchline of this Letter. We calculate the one- and two-triplon contribution of the dynamic structure factor (DSF) at $T = 0$ of two-leg QSLs in the presence of quenched bond disorder. It is demonstrated that disorder has huge effects on collective excitations yielding intriguing quantum structures directly relevant for spectroscopic experiments.

Disordered QSL.—The Hamiltonian of the disordered QSL for a fixed disorder configuration $\{J\}$ is given by

$$\mathcal{H}(\{J\}) = \sum_{\nu} \left(J_{\nu}^{\perp} \vec{S}_{\nu,1} \cdot \vec{S}_{\nu,2} + \sum_{n=1}^{2} J_{\nu,n}^{\parallel} \vec{S}_{\nu,n} \cdot \vec{S}_{\nu+1,n} \right), \tag{1}$$

where the sum runs over all rungs and $n = 1, 2$ denotes the legs of the QSL [see Fig. 1(a)]. The disorder configuration $\{J\}$ given by the antiferromagnetic $J_{\nu}^{\perp}$ and $J_{\nu,n}^{\parallel}$ depends on the type of quenched disorder. Here we focus on bimodal disorder; i.e., the rung and leg exchanges can take either the value J_1^{κ} with probability p or J_2^{κ} with probability $1 - p$ for $\kappa \in \{\perp, \parallel\}$. However, our technical treatment is more general and allows us to consider any stationary quenched bond disorder distribution.

Clean QSLs with $J_{\nu}^{\perp} \equiv J^{\perp}$ and $J_{\nu,n}^{\parallel} \equiv J^{\parallel}$ have an unordered ground state and gapped triplon excitations for all $J^{\parallel}/J^{\perp}$, which are adiabatically connected to the isolated rung limit $J^{\parallel} = 0$. In this limit the ground state is a product

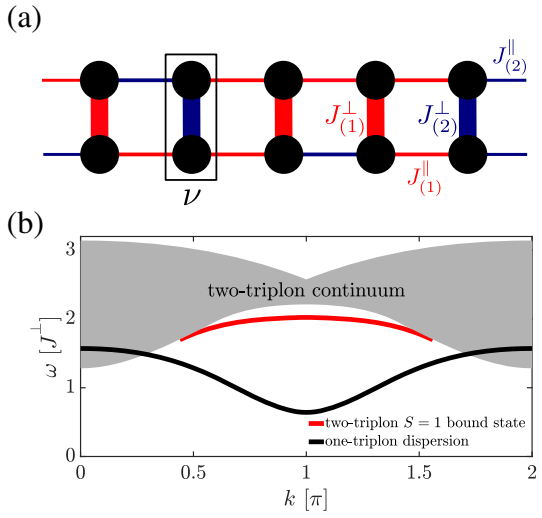

FIG. 1. (a) QSL with bimodal disorder. The two different rung ($J^{\perp}_{(1,2)}$) and leg ($J^{\parallel}_{(1,2)}$) couplings are shown as red and blue bonds. The unit cell ν is indicated by the rectangular box. (b) Spectrum of the clean QSL for $J^{\parallel}/J^{\perp} = 1/2$ as a function of momentum k including one-triplon dispersion (black line), two-triplon continuum (gray), as well as spin-one two-triplon bound state (red line) calculated by perturbative continuous unitary transformations (pCUTs).

state of singlets $|s\rangle = (|\uparrow\downarrow\rangle - |\downarrow\uparrow\rangle)/\sqrt{2}$ and excitations are local triplets $|t^{+1}\rangle = |\uparrow\uparrow\rangle$, $|t^{+0}\rangle = (|\uparrow\downarrow\rangle + |\downarrow\uparrow\rangle)/\sqrt{2}$, and $|t^{-1}\rangle = |\downarrow\downarrow\rangle$. The low-energy spectrum of the clean QSL obtained by pCUTs is shown for $J^{\parallel}/J^{\perp} = 1/2$ in Fig. 1(b). The spin-one triplon corresponds to a dressed triplet which has a finite cosinelike dispersion in this parameter regime with a finite gap at $k = \pi$. Two-triplon energies are either part of the two-triplon continuum or correspond to two-triplon (anti)-bound states, whose energies depend on the total spin. We focus on the spin-one sector, which is relevant for the DSF, where a two-triplon bound state exists for a large range of momenta in the clean QSL due to the attractive two-triplon interaction [38,39].

We then reformulate Eq. (1) in terms of triplet creation and annihilation operators $t^{(\dagger)}_{\nu,\alpha}$ with $t^{\dagger}_{\nu,\alpha}|s\rangle \equiv |t^{\alpha}\rangle$ and $\alpha \in \{\pm 1, 0\}$ on rung ν. Setting the average rung exchange $\bar{J}^{\perp} \equiv (J^{\perp}_1 + J^{\perp}_2)/2 \equiv 1$ and introducing the deviations $\Delta\bar{J}^{\perp}_{\pm}$ from it, allows us to express Eq. (1) as

$$\mathcal{H}(\{J\}) = E_0 + \mathcal{Q} + \sum_{n=-2}^{2} \hat{T}_n(\{J\}), \tag{2}$$

where $E_0 = -3/4(\mathcal{N}_r + \sum_{\nu}\Delta J^{\perp}_{\nu})$ with $\mathcal{N}_r$ the number of rungs, the counting operator $\mathcal{Q} = \sum_{\nu,\alpha}\hat{n}_{\nu,\alpha}$ with $\hat{n}_{\nu,\alpha} = t^{\dagger}_{\nu,\alpha}t_{\nu,\alpha}$, and the $\hat{T}_n$ with $[\hat{T}_n, \mathcal{Q}] = n\hat{T}_n$ change the triplet number by n [45]. The $\hat{T}_n$ depend explicitly on $\Delta\bar{J}^{\perp}_{\pm}$ as well as $J^{\parallel}_{1,2}$ and therefore on the disorder configuration $\{J\}$. Here $\hat{T}_{\pm 2}$ correspond to pair creation and annihilation processes, $\hat{T}_0$ contains triplet hopping as well as quartic triplet-triplet interactions, and $\hat{T}_{\pm 1}$ represent decay processes of one triplet into two or vice versa. Note that $\hat{T}_{\pm 1} = 0$ holds for the clean case where the QSL possesses an exact reflection symmetry about the centerline giving rise to a conserved parity quantum number ± 1.

The central quantity for inelastic neutron scattering on disordered QSLs is the disorder averaged DSF

$$S_{\pm}(k,\omega) \equiv \lim_{\mathcal{N}_{\rm dc}\to\infty} \frac{1}{\mathcal{N}_{\rm dc}} S_{\pm}(k,\omega,\{J\}), \tag{3}$$

with momentum k, frequency ω, number of disorder configurations $\mathcal{N}_{\rm dc}$, and

$$S_{\pm}(k,\omega,\{J\}) \equiv -\frac{1}{\pi}\mathrm{Im}\langle 0|\mathcal{O}^{\dagger}_{\pm}\frac{1}{\omega - \mathcal{H} + i0^{+}}\mathcal{O}_{\pm}|0\rangle, \tag{4}$$

where $\mathcal{O}_{\pm}(k) \equiv \sum_{\nu} e^{ik\nu}(S^z_{\nu,1} \pm S^z_{\nu,2})/(2\sqrt{\mathcal{N}_r})$. The index $\pm$ reduces to the parity quantum number for the clean QSL.

pCUT.—We perform pCUTs [50,51] as our main approach as well as bond-operator MF theory (for the latter see Ref. [45]). The major target of a pCUT is to unitarily transform Eq. (2), order by order in $J^{\parallel}_{\nu,n}$ and $\Delta\bar{J}^{\perp}_{\pm}$, to an effective Hamiltonian $\mathcal{H}_{\rm eff}$ which conserves the number of triplons so that $[\mathcal{H}_{\rm eff}, \mathcal{Q}] = 0$ holds. As a consequence, the complicated quantum many-body system is mapped to an effective few-body problem which is easier to solve. A pCUT application has a model-independent step, which expresses $\mathcal{H}_{\rm eff}$ in a sum of operator product sequences of the $\hat{T}_n$ operators with exactly known coefficients. The most efficient way of performing the second model-dependent step, which amounts to normal order $\mathcal{H}_{\rm eff}$, is a full-graph decomposition using the linked-cluster theorem. Here the only graphs are ladders segments so that the calculation for the clean QSL is very simple. In contrast, in the presence of bimodal disorder, there are $2^{3\mathcal{N}_r+1}$ different graphs for a ladder segment of $\mathcal{N}_r$ rungs and a linked-cluster expansion becomes unefficient since $\mathcal{N}_{\rm dc}$ is large. At this point white graphs [52] are essential, since it allows to specify $\{J\}$ only *after* the calculations on the graphs. In practice, one determines the most general linked contribution of a graph by allowing for a different exchange coupling on every nearest-neighbor link of the graph. The resulting multivariable series can then be embedded on any specific $\{J\}$.

We calculated $\mathcal{H}_{\rm eff}$ in the one- and two-triplon sector up to order 8 and we determined the corresponding effective observables $\mathcal{O}^{\rm eff}_{\pm}$ up to order 7. The convergence of the bare series is similar to the clean QSL where it gives quantitative results up to $J^{\parallel}/J^{\perp} \lesssim 0.5$ [39,40] and we therefore restrict to this parameter regime below. The effective one- and two-triplon problem is then diagonalized for finite QSLs with $\mathcal{N}_r = 100$ and the DSF for a fixed disorder configuration is obtained using a finite broadening $\Gamma = 0.01$. Averaging over $\mathcal{N}_{\rm dc} = 1000$ disorder configurations then gives the

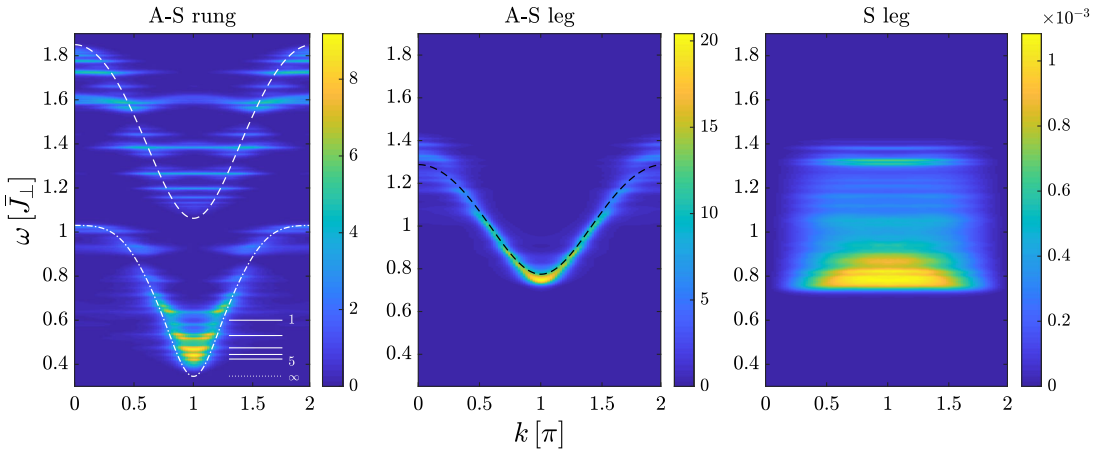

FIG. 2. One-triplon contribution to the antisymmetric DSF $S_-(k,\omega)$ for pure rung (A-S rung) or leg (A-S leg) disorder and to the symmetric DSF $S_+(k,\omega)$ for pure leg disorder (S leg). *A-S rung*: bimodal rung disorder with $p = 0.5$ and rung exchanges $J_1^\perp = 1.4$ and $J_2^\perp = 0.6$. The constant leg exchange is $J^\parallel = 0.4$. White lines represent one-triplon dispersions for a clean QSL with $J^\parallel = 0.4$ and $J^\perp = 1.4$ (dashed) or $J^\perp = 0.6$ (dashed-dotted). Horizontal white lines indicate the lowest one-triplon energy $\epsilon_1^{(L)}$ of open ladder segments of length L with $J^\perp = 0.6$. *A-S/S leg*: bimodal leg disorder with $p = 0.5$ and leg exchanges $J_1^\parallel = 0.1$ and $J_2^\parallel = 0.4$. The black dashed line represents the one-triplon dispersion with mean hopping amplitudes.

averaged DSF (3). All relevant aspects discussed below are well converged despite the use of finite $\mathcal{N}_\mathrm{r}$ and $\mathcal{N}_\mathrm{dc}$ [45], which is reasonable due to the finite localization and correlation length of the QSL.

One-triplon contribution.—For the clean QSL, this sector can be expressed as $S_-(k,\omega) = a^2(k)\delta(\omega - \omega_k)$ with the one-triplon dispersion ω_k and the one-triplon spectral weights $a^2(k)$ while $S_+(k,\omega) = 0$ due to the parity symmetry. The dispersion ω_k is cosine shaped with gap at $k = \pi$ and the spectral weight $a^2(k)$ is monotonic in k with maximum at $k = \pi$ and minimum at $k = 0$.

Representative pCUT results for the DSF in the presence of the maximal pure rung or leg disorder are shown in Fig. 2 (see Ref. [45] for qualitatively the same MF results). These two cases behave differently with respect to reflection about the centerline. For rung disorder the associated parity is still a conserved quantity and therefore $S_+(k,\omega) = 0$ holds for the one-triplon sector. In contrast, since the leg disorder breaks the reflection symmetry, a finite one-triplon contribution to $S_+(k,\omega)$ exists. However, this contribution is orders of magnitude smaller and the dominant contribution to the DSF is still $S_-(k,\omega)$. We find that the DSF of the disordered QSLs is fundamentally different to the one for the clean counterpart. These differences do not originate from large changes of the spectral weights. Indeed, deviations to a clean QSL with constant mean exchange couplings are small [45]. Certainly, the most important effect of disorder on the DSF is the disorder-induced localization of eigenfunctions and their corresponding shape changes in momentum space. Furthermore, the density of states is changed by the bimodal disorder [45].

There are fundamental differences between leg and rung disorder, although eigenfunctions are localized in both cases. This is understood in leading-order perturbation theory: rung disorder leads to triplons hopping in a disordered chemical potential while leg disorder yields a disordered nearest-neighbor hopping and therefore to a momentum-dependent disorder potential. Thus localization is stronger for rung compared to leg disorder.

We find two separated energy regions for rung disorder corresponding to $J_1^\perp$ and $J_2^\perp$. This can be seen by comparing to the one-triplon dispersions of a clean QSL with these $J_\nu^\perp$ (white lines in Fig. 2). In first order this follows from Gershgorin's circle theorem which states that half of the eigenvalues are bigger and half of them smaller than one in the thermodynamic limit for this specific disorder.

The spectral weights are higher in the low-energy region due to localization. Considering an eigenstate in the lower (higher) region, it will be localized around states with dominantly low (high) rung values. For the eigenstates in the low-energy region the average ratio of leg and rung coupling is therefore larger. Hence the spectral weight is larger in the low-energy region. Most importantly, we observe a fragmentation of the one-triplon DSF into energies carrying maximal spectral weights close to $k = \pi$. These energies with largest intensity are located well above the one-triplon gap of the uniform QSL with the lower rung value and can be understood by considering leading-order degenerate perturbation theory for small $J^\parallel/\Delta\bar{J}^\perp$ [45]. In this limit one has a fragmentation of the disordered QSL into decoupled ladder segments with constant $J^\perp = 0.6$ of length L. In each open segment one can easily solve the full one-triplon problem and determine the lowest one-triplon energy $\epsilon_1^{(L)}$. For $k = \pi$, we find that the one-triplon DSF has indeed local intensity maxima at these energies (see solid white lines in Fig. 2).

The approximate quantization of the one-triplon DSF is therefore directly linked to the discrete energies $\epsilon_1^{(L)}$ arising from the strong rung disorder. Note that similar quantum structures occur also for the high-energy region of the one-triplon DSF which can be again traced back to a fragmentation of the disordered QSL into almost decoupled ladder segments. For leg disorder one has only a single energy region which is well described with a one-triplon dispersion using mean hopping amplitudes (black line in Fig. 2). The spectral weight is largest at $k = \pi$ and diminishes towards $k = 0$. However, the intensities are even smaller at small k as one expects from the spectral weight, since it is distributed over a particularly broad range of energies at $k = 0$. This comes from disorder in the local hopping amplitude (like for rung disorder) which appears in subleading orders leading to an anisotropy between $k = 0$ and $k = \pi$ [45]. Further, the fragmentation at $k = 0$ is of similar origin as for rung disorder found for all momenta. Finally, the shape of the one-triplon contribution to $S_+(k,\omega)$ can be fully traced back to the different type of observable. Although the spectral weight vanishes exactly at $k = 0$, it is distributed almost uniformly between $k = \pi/2$ and $k = \pi$ [45]. The same is true for the intensities at fixed energy. For the latter one has to recapitulate that the local observable in real space only injects a finite weight for single triplons if an asymmetry of leg couplings is present in the local surrounding of the observable. The probability of such an asymmetric and connected region of length L, where $\mathcal{O}_+(k)$ is active, is exponentially descreasing with L. It follows that the projection of eigenstates on these regions is almost flat in momentum space.

Two-triplon contribution.—For the clean QSL, it is contained solely in $S_+(k,\omega)$ while $S_-(k,\omega) = 0$. It comprises a continuum and a two-triplon bound state [see Fig. 1(b)]. By far most of the spectral weight is carried by this bound state, which therefore dominates the DSF.

The two-triplon contributions obtained by pCUTs with maximal pure rung or leg disorder are shown in Fig. 3. Note that bond-operator MF does not yield satisfactory results in this sector, since the attractive triplon interaction is neglected completely [45]. Localization also occurs for two-triplon states so that eigenstates have almost all their weight on a finite part of the two-triplon space in the position basis [45]. Further, the states carrying most of the weight will be two-triplon states localized on a finite region of the lattice. For rung disorder, there are three possible values for the sum of two local hopping amplitudes resulting in three distinct structures in the DSF. The spectral weight of these structures decreases from lower to higher energy, which can be understood from the decreasing average ratio of leg and rung couplings as described for the one-triplon case above. Each region contains a bound state and a continuum, although only the bound state carries significant spectral weight (see Fig. 3, left). They gain a finite lifetime due to the disorder. The same is true for leg disorder. One observes two bound-state structures, which fuse at $k = \pi$. The two structures, one more dispersive than the other, can be linked to the bound states of clean QSLs taking the larger or lower leg coupling (see Fig. 3, middle). Interestingly, the maximal weight at $k = \pi$ is located at a lower energy compared to the bound states of the clean QSLs. This is likely caused by scattering events of lower-energy bound states with $k < \pi$ yielding a final momentum $k = \pi$. Finally, the two-triplon contribution to $S_-(k,\omega)$ (see Fig. 3, right), which is induced by the leg disorder, has an order of magnitude larger weight compared to the one-triplon contribution to $S_+(k,\omega)$ although the shape is similar. Notably, the maximum

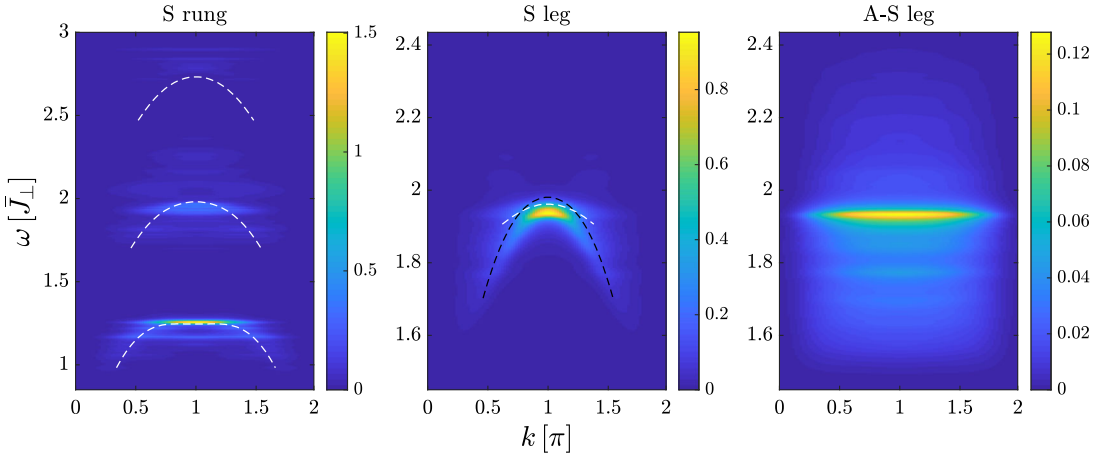

FIG. 3. Two-triplon contribution to the symmetric DSF $S_+(k,\omega)$ for pure rung (S rung) or leg (S leg) disorder and to the antisymmetric DSF $S_-(k,\omega)$ for pure leg disorder (A-S leg). *S rung*: bimodal rung disorder with $p = 0.5$ and rung exchanges $J_1^\perp = 1.4$ and $J_2^\perp = 0.6$. The constant leg exchange is $J^\parallel = 0.4$. The three dashed lines represent the dispersion of the two-triplon bound state for the clean QSL using $J^\perp = 1.4$, $J^\perp = 1.0$, and $J^\perp = 0.6$. *S/A-S leg*: bimodal leg disorder with $p = 0.5$ and leg exchanges $J_1^\parallel = 0.1$ and $J_2^\parallel = 0.4$. The dashed lines represent the dispersion of the two-triplon bound state for the clean QSL with $J_1^\parallel$ (white) and $J_2^\parallel$ (black).

intensity is at the same energy as for $S_+(\pi,\omega)$ and is again associated with bound states.

Conclusions.—The pCUT method is an efficient tool to investigate the fate of quasi-particles under quenched disorder, which we exemplified by calculating the DSF of disordered QSLs. Disorder-induced quantum structures like the quantization of collective triplon excitations in the DSF emerge which are of direct relevance for spectroscopic experiments. We therefore suspect that our findings trigger experimental as well as further theoretical investigations on the fate of quasi-particles in disordered correlated quantum matter.

We thank Bruce Normand and Christian Rüegg for fruitful discussions. M. H. and K. P. S. acknowledge financial support from DFG Project No. SCHM 2511/10-1.

*max.hoermann@fau.de
†paul.wunderlich@fau.de
‡kai.phillip.schmidt@fau.de

[1] T. Vojta, J. Phys. A **39**, R143 (2006).
[2] T. Vojta, J. Low Temp. Phys. **161**, 299 (2010).
[3] R. B. Griffith, Phys. Rev. Lett. **23**, 17 (1969).
[4] D. M. Basko, I. L. Aleiner, and B. L. Altshuler, Ann. Phys. (Amsterdam) **321**, 1126 (2006).
[5] V. Oganesyan and D. A. Huse, Phys. Rev. B **75**, 155111 (2007).
[6] M. Znidaric, T. Prosen, and P. Prelovsek, Phys. Rev. B **77**, 064426 (2008).
[7] A. Pal and D. A. Huse, Phys. Rev. B **82**, 174411 (2010).
[8] A. Furusaki, M. Sigrist, P. A. Lee, K. Tanaka, and N. Nagaosa, Phys. Rev. Lett. **73**, 2622 (1994).
[9] E. Westerberg, A. Furusaki, M. Sigrist, and P. A. Lee, Phys. Rev. Lett. **75**, 4302 (1995).
[10] N. Nagaosa, A. Furusaki, M. Sigrist, and H. Fukuyama, J. Phys. Soc. Jpn. **65**, 3724 (1996).
[11] T. Miyazaki, M. Troyer, M. Ogata, K. Ueda, and D. Yoshioka, J. Phys. Soc. Jpn. **66**, 2580 (1997).
[12] M. Greven and R. J. Birgeneau, Phys. Rev. Lett. **81**, 1945 (1998).
[13] R. Mélin, Y.-C. Lin, P. Lajko, H. Rieger, and F. Igloi, Phys. Rev. B **65**, 104415 (2002).
[14] J. A. Hoyos and E. Miranda, Phys. Rev. B **69**, 214411 (2004).
[15] K. Trinh, S. Haas, R. Yu, and T. Roscilde, Phys. Rev. B **85**, 035134 (2012).
[16] K. Trinh and S. Haas, Phys. Rev. B **87**, 075137 (2013).
[17] H. Manaka, A. V. Kolomiets, and T. Goto, Phys. Rev. Lett. **101**, 077204 (2008).
[18] H. Manaka, H. A. Katori, O. V. Kolomiets, and T. Goto, Phys. Rev. B **79**, 092401 (2009).
[19] T. Hong, A. Zheludev, H. Manaka, and L.-P. Regnault, Phys. Rev. B **81**, 060410 (2010).
[20] M. B. Stone, A. Podlesnyak, G. Ehlers, A. Hug, E. C. Samulon, M. C. Shapiro, and I. R. Fisher, J. Phys. Condens. Matter **23**, 416003 (2011).
[21] D. Hüvonen, S. Zhao, M. Mansson, T. Yankova, E. Ressouche, C. Niedermayer, M. Laver, S. N. Gvasaliya, and A. Zheludev, Phys. Rev. B **85**, 100410 (2012).
[22] D. Hüvonen, S. Zhao, G. Ehlers, M. Mansson, S. N. Gvasaliya, and A. Zheludev, Phys. Rev. B **86**, 214408 (2012).
[23] B. Nafradi, T. Keller, H. Manaka, U. Stuhr, A. Zheludev, and B. Keimer, Phys. Rev. B **87**, 020408 (2013).
[24] K. Y. Povarov, E. Wulf, D. Hüvonen, J. Ollivier, A. Paduan-Filho, and A. Zheludev, Phys. Rev. B **92**, 024429 (2015).
[25] O. Motrunich, K. Damle, and D. A. Huse, Phys. Rev. B **63**, 134424 (2001).
[26] M. Vojta, Phys. Rev. Lett. **111**, 097202 (2013).
[27] Y.-R. Shu, M. Dupont, D.-X. Yao, S. Capponi, and A. W. Sandvik, Phys. Rev. B **97**, 104424 (2018).
[28] E. Dagotto and T. M. Rice, Science **271**, 618 (1996).
[29] M. Windt, M. Grüninger, T. Nunner, C. Knetter, K. P. Schmidt, G. S. Uhrig, T. Kopp, A. Freimuth, U. Ammerahl, B. Büchner, and A. Revcolevschi, Phys. Rev. Lett. **87**, 127002 (2001).
[30] S. Notbohm, P. Ribeiro, B. Lake, D. A. Tennant, K. P. Schmidt, G. S. Uhrig, C. Hess, R. Klingeler, G. Behr, B. Büchner, M. Reehuis, R. I. Bewley, C. D. Frost, P. Manuel, and R. S. Eccleston, Phys. Rev. Lett. **98**, 027403 (2007).
[31] Ch. Rüegg, K. Kiefer, B. Thielemann, D. F. McMorrow, V. Zapf, B. Normand, M. B. Zvonarev, P. Bouillot, C. Kollath, T. Giamarchi, S. Capponi, D. Poilblanc, D. Biner, and K. W. Krämer, Phys. Rev. Lett. **101**, 247202 (2008).
[32] T. Hong, Y. H. Kim, C. Hotta, Y. Takano, G. Tremelling, M. M. Turnbull, C. P. Landee, H.-J. Kang, N. B. Christensen, K. Lefmann, K. P. Schmidt, G. S. Uhrig, and C. Broholm, Phys. Rev. Lett. **105**, 137207 (2010).
[33] S. Ward, P. Bouillot, H. Ryll, H. Kiefer, K. W. Krämer, Ch. Rüegg, C. Kollath, and T. Giamarchi, J. Phys. Condens. Matter **25**, 014004 (2013).
[34] D. Schmidiger, P. Bouillot, T. Guidi, R. Bewley, C. Kollath, T. Giamarchi, and A. Zheludev, Phys. Rev. Lett. **111**, 107202 (2013).
[35] S. Ward, M. Mena, P. Bouillot, C. Kollath, T. Giamarchi, K. P. Schmidt, B. Normand, K. W. Krämer, D. Biner, R. Bewley, T. Guidi, M. Boehm, D. F. McMorrow, and Ch. Rüegg, Phys. Rev. Lett. **118**, 177202 (2017).
[36] T. Barnes, E. Dagotto, J. Riera, and E. S. Swanson, Phys. Rev. B **47**, 3196 (1993).
[37] D. G. Shelton, A. A. Nersesyan, and A. M. Tsvelik, Phys. Rev. B **53**, 8521 (1996).
[38] S. Trebst, H. Monien, C. J. Hamer, Z. Weihong, and R. R. P. Singh, Phys. Rev. Lett. **85**, 4373 (2000).
[39] C. Knetter, K. P. Schmidt, M. Grüninger, and G. S. Uhrig, Phys. Rev. Lett. **87**, 167204 (2001).
[40] K. P. Schmidt, C. Knetter, and G. S. Uhrig, Eur. Phys. Lett. **56**, 877 (2001).
[41] A. Lauchli, G. Schmid, and M. Troyer, Phys. Rev. B **67**, 100409 (2003).
[42] K. P. Schmidt and G. S. Uhrig, Phys. Rev. Lett. **90**, 227204 (2003).
[43] D. Schmidiger, K. Y. Povarov, S. Galeski, N. Reynolds, R. Bewley, T. Guidi, J. Ollivier, and A. Zheludev, Phys. Rev. Lett. **116**, 257203 (2016).

[44] S. Ward, Ph.D. thesis, University College London, 2014.
[45] See Supplemental Material at http://link.aps.org/supplemental/10.1103/PhysRevLett.121.167201 for detailed information on the improved bond-operator mean-field theory and corresponding results for the DSF, the momentum dependence of momentum state lifetimes, a detailed discussion of the leading-order effects for rung disorder, pCUT results for the spectral weight, density of states, and inverse participation ratio, as well as the convergence properties of the pCUT approach. The Supplemental Material contains Refs. [46–49].
[46] S. Gopalan, T. M. Rice, and M. Sigrist, Phys. Rev. B **49**, 8901 (1994).
[47] B. Normand and Ch. Rüegg, Phys. Rev. B **83**, 054415 (2011).
[48] D. J. Thouless, Phys. Rep. **13**, 93 (1974).
[49] S. Sachdev and R. N. Bhatt, Phys. Rev. B **41**, 9323 (1990).
[50] C. Knetter and G. S. Uhrig, Eur. Phys. J. B **13**, 209 (2000).
[51] C. Knetter, K. P. Schmidt, and G. S. Uhrig, J. Phys. A **36**, 7889 (2003).
[52] K. Coester and K. P. Schmidt, Phys. Rev. E **92**, 022118 (2015).